ECOHYDROLOGY
Ecohydrol. (2014)
Published online in Wiley Online Library
(wileyonlinelibrary.com) DOI: 10.1002/eco.1472

Soil clay influences *Acacia* encroachment in a South African grassland

Séraphine Grellier,[1]* Nicolas Florsch,[2] Jean-Louis Janeau,[3] Pascal Podwojewski,[4,5] Christian Camerlynck,[6] Sébastien Barot,[7] David Ward[8] and Simon Lorentz[5]

[1] *University of Science and Technology of Hanoi (USTH), 18 Hoang Quoc Viet, Cau Giay, Hanoi, Vietnam*
[2] *Sorbonne Universités, UPMC Univ Paris 06, UMI 209, UMMISCO, F-75005, Paris, France*
[3] *IRD-BIOEMCO c/o Soils and Fertilisers Research Institute (SFRI), Dong Ngac, Chem, Tu Liem District, Hanoi, Vietnam*
[4] *IRD-BIOEMCO, 32, av. H. Varagnat, 93143, Bondy cedex, France*
[5] *Center for Water Resources Research, University of KwaZulu-Natal, Box X01, Scottsville 3209, South Africa*
[6] *Sorbonne Universités, UPMC Univ Paris 06, UMR 7619 Metis, F-75005, Paris, France*
[7] *IRD-BIOEMCO, Ecole Normale Supérieure, 46 rue d'Ulm, 75230, Paris 05, France*
[8] *School of Life Sciences, University of KwaZulu-Natal, Box X01, Scottsville 3209, South Africa*

ABSTRACT

Because of technical difficulties in measuring soil properties at a large scale, little is known about the effect of soil properties on the spatial distribution of trees in grasslands. We were interested in the associations of soil properties with the phenomenon of tree encroachment, where trees increase in density at the expense of grasses. The spatial variation of soil properties and especially soil texture may modify the properties of hydraulic conductivity, and the availability of soil water and mineral nutrients, which in turn may affect the spatial distribution of encroaching trees. Through the development of a geophysical method (Slingram) using an electromagnetic device EM38 and Bayesian inversion, we were able to accurately map soil electrical conductivity (EC) of a Luvisol in a grassland of South Africa. EC measured at the 0·8 to 2 m depth on a 1·5 ha area is a proxy for clay content and was correlated with the spatial distribution of four size classes of the encroaching *Acacia sieberiana*. Tree location (all sizes considered) was significantly correlated with EC. Tall acacias (>3m height) were totally absent from patches with EC >24 mS m^{-1}. For all other size classes from medium trees to seedlings, tree density decreased with increasing EC. This suggests that high clay contents at depth associated with high EC values may prevent the establishment and/or survival of trees and influence the spatial distribution of *A. sieberiana*. This result also shows that geophysical tools may be useful for demonstrating important ecological processes. Copyright © 2014 John Wiley & Sons, Ltd.

KEY WORDS *Acacia sieberiana*; Bayesian inversion; conductivity; EM38; geophysics; Slingram method; soil horizon; woody plant encroachment

Received 23 August 2013; Revised 7 January 2014; Accepted 7 January 2014

INTRODUCTION

Woody plant encroachment in grassland has been widely studied (Archer, 1995; Brown and Archer, 1999; Sankaran *et al*., 2005; Ward, 2005; Sankaran *et al*., 2008; Van Auken, 2009). The main factors controlling this phenomena are the availability of resources (water, nutrients), fires, herbivory (Sankaran *et al*., 2004) and possibly global climate changes (Bond and Midgley, 2000; Ward, 2010). Scientists have only recently started to explore the factors controlling the spatial pattern of encroaching tree populations (Wiegand *et al*., 2006; Halpern *et al*., 2010; Robinson *et al*., 2010). However, a better understanding of these patterns would give new insights into the complex issue of the mechanisms leading to encroachment (Ward, 2005; Graz, 2008). Various models have been proposed, including spatially explicit models (Wiegand *et al*., 2005; Wiegand *et al*., 2006; Meyer *et al*., 2007) where trees are aggregated in patches whose dynamics are driven mainly by rainfall and inter-tree competition with a shift between facilitation and competition (Callaway and Walker, 1997; Halpern *et al*., 2010). Soil nutrient patches have also been highlighted as driving spatial patterns of palm trees in tropical humid savanna of Lamto in the Ivory Coast (Barot *et al*., 1999). The opposite relationship, i.e. herbaceous or woody vegetation modifying soil properties and ecosystem functioning, has also been demonstrated (Lata *et al*., 2004; Grellier *et al*., 2013b; Verboom and Pate, 2013). If other studies mentioned the importance of soil properties on dynamics of woody vegetation (Britz and Ward, 2007; Schleicher *et al*., 2011), few have tested the effects

*Correspondence to: Séraphine Grellier, University of Science and Technology (USTH), 18 Hoang Quoc Viet, Cau Giay, Hanoi, Vietnam.
E-mail: seraphine.grellier@usth.edu.vn

of soil properties on vegetation spatial pattern in grasslands (Browning *et al.*, 2008; Eggemeyer and Schwinning, 2009; Robinson *et al.*, 2010; Colgan *et al.*, 2012). Spatial variations in soil properties and especially soil texture may modify the availability of soil moisture (Weng and Luo, 2008; Wang *et al.*, 2012), the availability of mineral nutrients (Bechtold and Naiman, 2006) and hydraulic conductivity (Corwin and Lesch, 2005). All these factors may affect the spatial distribution of vegetation (Robinson *et al.*, 2010).

The lack of studies addressing this type of issue is probably due to technical issues of measuring soil properties at the landscape scale. The recent interdisciplinary links between soil science, hydrology and ecology (Young *et al.*, 2010) offer useful possibilities for throwing new light on this issue by taking into account more factors that could be missed otherwise. Within this framework, Robinson *et al.* (2008) considered geophysical methods for mapping soil properties at the watershed scale and related them to vegetation spatial patterns.

In this study, we explore the relationships between the spatial pattern of trees and soil properties such as clay content through geophysical measurements. As roots of adult and young trees reach different soil layers (Grellier, 2011) and because different processes affect their growth (Callaway and Walker, 1997; Grellier *et al.*, 2012a), we may find differences between the spatial distributions of size classes of trees. We focused on *Acacia sieberiana*, which encroaches grasslands of KwaZulu-Natal in South Africa. The main questions that we aimed to answer are as follows:

1. Does the spatial pattern of acacias depend on soil properties (particularly clay content) at different depths?
2. Does this pattern change with *Acacia* size?

We answer these two questions by studying the relationship between tree location according to tree size on a 1·5ha area and measured electrical conductivity (EC) of soil linked to the clay content of a two-layered shallow soil, e.g. a topsoil at 0–0·8 m (upper layer) and a subsoil at 0·8–2 m (lower layer). We used the non-destructive Slingram method to characterize the EC of the first 2 m of soil. This method has often been used to study interactions between plants and soils (Myers *et al.*, 2007; Hossain *et al.*, 2010). A previous study (Grellier *et al.*, 2013a), dedicated to methodology, validated the geophysical method, which was used and was simplified in this study to assess our ecological questions regarding tree encroachment (cf. Discussion Section).

MATERIALS AND METHODS

Description of the study site

We conducted the study in a communal grassland of the Potshini village (28° 48′ 37″ S; 29° 21′ 19″ E), Kwazulu-Natal province, South Africa (Figure 1). The average altitude of the selected area of 1·5 ha (100 m × 150 m) was 1305 m a.s.l. The climate is sub-humid sub-tropical with four seasons, of which two are well marked: wet summer (October to April) and dry winter (May to September). The mean annual precipitation calculated from 1945 to 2009 was 750 mm (Grellier *et al.*, 2012b). The mean annual temperature in 2008 and 2009 was 16·3 °C. This site belongs to the Northern KwaZulu-Natal moist grassland biome (Mucina and Rutherford, 2006). Encroachment by a single indigenous tree species, *A. sieberiana* var. *woodii* (Burtt Davy) Keay & Brenan, has occurred in the valley for the last 30 years (Grellier *et al.*, 2012b). The geology of the site is characterized by fine-grained sandstones, shales, siltstone and mudstones that alternate in horizontal succession and belong to the Beaufort and Ecca Groups of the Karoo Supergroup (King, 2002). Unconsolidated colluvial polycyclic deposits up to 15 m thick from the Pleistocene fill the valleys and are very prone to linear gully erosion (Botha *et al.*, 1994). The general soil type is Luvisol (FAO, 1998) with three well-delimited main horizons. The A horizon (between 0 and 40–50 cm) is coherent, loamy texture with brown colour (10 yr 4/1 to 10 yr 4/3). The Bt Horizon (from 40–50 to 70 cm) is dark brown (5–10 yr 4/2), clay-loamy, very coherent and hard with a coarse blocky structure. The C horizon below 80cm depth is a Pleistocenic colluvium 0·30–5 m thick, brown (7·5 yr 4/6 to 5/6) sandy clay loam, not well structured, prone to dispersion. This layer could be considered as a Paleosol. The clay mineralogy is exclusively Illite in the A and Bt horizon and an interstratified illite/illite-smectite in the C horizon. Evidence of lepidocrocite, mineral typical of temporary water-logging appear just above the Bt horizon (comm. pers. P. Podwojewski).

Topsoil and subsoil electrical conductivity measurement with the Slingram EM38 device

The Slingram method for water and clay content assessment has been applied by several authors (Cockx *et al.*, 2007; Hezarjaribi and Sourell, 2007). The general principle of the Slingram EM38 device is well described by McNeill (1980). To summarize, one coil serves as a transmitter and produces an alternative magnetic field in the ground (14·6 kHz for the EM38-MK2 used here). This primary magnetic field induces an electric field E as stated by Maxwell–Faraday's equation. The induced electric field leads to a current density $\rightarrow J$ according to Ohm's law $\rightarrow J = \sigma \rightarrow E$, where σ is the EC. These currents produce a secondary magnetic field following Maxwell–Ampere's equation. The former is detected by the second coil (receiver) and is electronically separated from the primary field. This secondary field directly reflects a mean conductivity weighted in the medium under the coils. The depth of investigation mainly depends not only on the coil separation but also on the direction of the coils' axes.

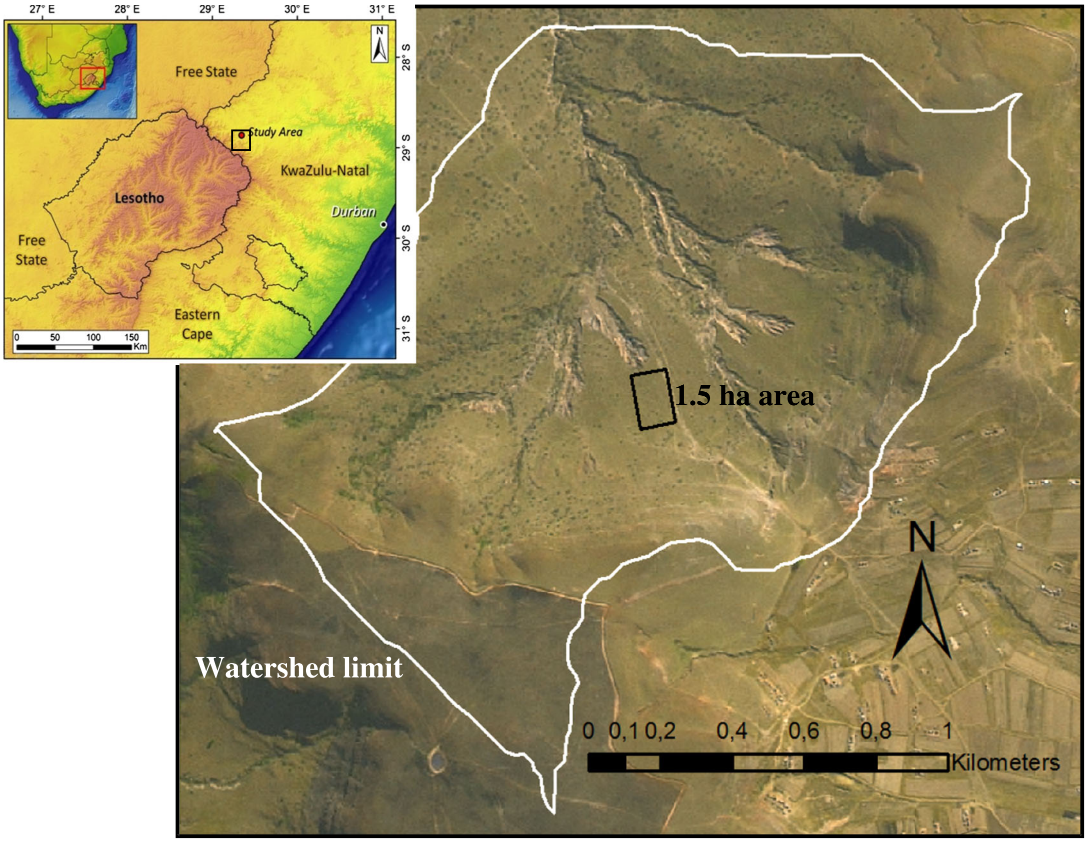

Figure 1. Location of the study site represented on an aerial photograph of 2008.

With the Geonics EM38-MK2 device we used in this study, two modes of measurement were applied to benefit from two different investigation depths: the vertical dipole mode in which the two coil axes are vertical and the horizontal mode where the axes are horizontal. Axes were separated by 1 m to avoid high sensitivity to ground roughness that arises with lower spacing. This was also adapted to the soil depth we particularly wanted to investigate (between the surface and 2 m depth, with a peak of sensitivity at 0·4 m in vertical mode and for the first 20 cm in horizontal mode). We measured conductivity in the 1·5 ha plot by taking readings at all intersections of a 5 × 5 m grid in both dry (June) and wet (February) seasons, applying appropriate calibration methods as described by Grellier *et al.* (2013a).

Electrical conductivity inversion scheme details

The method presented here uses the inversion method given in a previous study devoted to the methodology of the Bayesian inverse problem applied to Slingram data, using the Potshini area of KwaZulu-Natal as a sample site (Grellier *et al.*, 2013a). Initially, preliminary pit logging of resistivity and a set of Vertical Electrical Soundings lead us to distinguish the main geoelectrical layers, characterized by their large differences in EC. In this previous study (Grellier *et al.*, 2013a), we mapped the conductivities of the two layers including the depth of the interface, from the EM38 maps sampled over a 5 × 5 m grid. Both the 0·5 m and 1m coil spacings offered by the EM38 MK2 were used, providing four data at each point (two spacings, vertical and horizontal mode for each, with an accuracy of the measurement approximately 1 mS m^{-1}). After inversion, the first layer showed EC lying between 1 and 4 mS m^{-1} and more often between 1 and 2 mS m^{-1} during the dry season. The second layer was more conductive, showing lateral variation between 10 and 40 mS m^{-1}. In the present study, we retained this Bayesian approach but significantly simplified the procedure, using the lessons provided by this initial study. We used a simplified two-layer model to represent the soil EC in the first 2 m, in which the interface depth was fixed at $h = 0{\cdot}8$ m (Figure 2). Setting a value of the interface depth leads to robust conductivity estimations. Only two parameters need be retrieved. This is consistent with the fact that two data points are obtained by using the vertical and horizontal mode in the 1m spacing. Additionally, the widespread version of the EM38 (having only the 1m spacing available) is perfectly utilizable in that case, and the whole procedure leads to a robust and simple approach in the field.

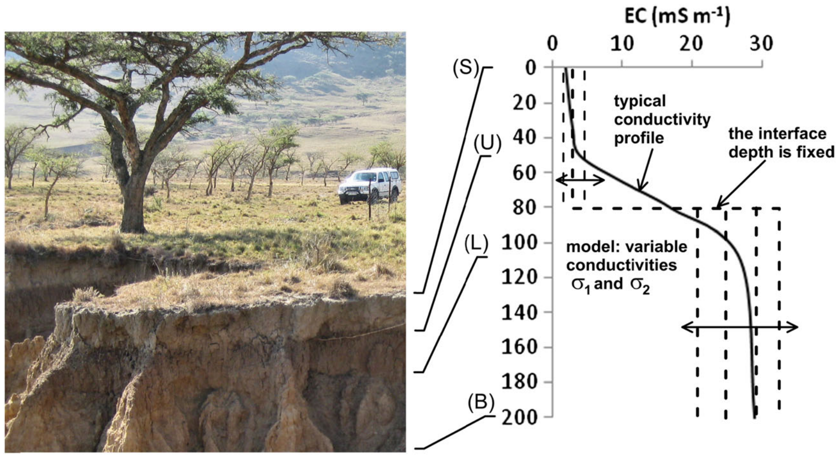

Figure 2. Photography of a gully side on the left and a typical electrical conductivity profile against depth (continuous curve) together with the fitted model used in this study (dotted lines) on the right. (S) surface; (U) upper limit of the transition layer; (L) lower limit of the transition layer; (B) conventional model bottom (=practical device sensitivity limit).

We consider the curve represented in Figure 2 as a representative EC profile of the study site. The first layer, 'topsoil', has an *a priori* low EC; the variability of the EC of the second layer can be attributed to clay content variability (Grellier *et al.*, 2013a). In the previous study with the full Bayesian approach, the measured EC indicates (after inversion) an interface depth varying from 0.4 to 1 m. Here, we chose $h = 0{\cdot}8$ m because it corresponds to the inflexion point of the 'typical' curve and it is also compatible with the uncertainties and the equivalence law applied here (Grellier *et al.*, 2013a). In this model involving a fixed depth, the conductivities are allowed to be free, and benefits from setting h in terms of robustness.

A sensibility analysis

How are the data sensitive and representative of the model two-layer conductivities? Assuming this simplified model, the EM38-MK2 1m spacing displays an 'apparent EC', which involves the two conductivities and the interface depth. This apparent EC in the vertical dipole mode and horizontal dipole mode, respectively, are given by McNeill (1980)

$$\begin{cases} \sigma_a^V = \sigma_1[1 - R_V] + \sigma_2 R_V \\ \sigma_a^H = \sigma_1[1 - R_H] + \sigma_2 R_H \end{cases} \tag{1}$$

where σ_1 and σ_2 are the conductivities of the topsoil and subsoil, respectively, and

$$\begin{cases} R_V = \dfrac{1}{\sqrt{4h^2 + 1}} \\ R_H = \sqrt{4h^2 + 1} - 2h \end{cases} \tag{2}$$

where h is the interface depth.

Since h is fixed, R_V and R_H are known, and Equation (1) becomes a simple 2×2 linear system with unknowns $\{\sigma_1, \sigma_2\}$. Notice, however, that this simple formula [as well as Equation (6)] cannot be used to process reliable inversion, without additional considerations, because of the strong correlation existing between the two conductivities. If one wanted to perform an inversion from this formula, we should take into account that these parameters are Jeffrey's type parameters and then one the conductivities must be replaced first by their logarithms in the inversion scheme, as follows:

$$\begin{cases} \sigma_a^V = e^{\Sigma_1}[1 - R_V] + e^{\Sigma_2} R_V \\ \sigma_a^H = e^{\Sigma_1}[1 - R_H] + e^{\Sigma_2} R_H \end{cases} \tag{3}$$

where

$$\Sigma_{1\ \mathrm{resp.}2} = \log\left(\sigma_{1\ \mathrm{resp.}2}\right) \tag{4}$$

The problem becomes nonlinear. A full inversion of Equation (3) requires introducing *a priori* information, and an algorithm capable of solving nonlinear problems, for instance, the recursive formula 23 of Tarantola and Valette (1982a). It is not used here, because we benefit from the full Bayesian approach, whereas the Tarantola and Valette method is 'encapsulated' in the Bayesian theory (also synthesized by Tarantola and Valette (1982b)). Additional points of view and justifications can be found in the work of Grellier *et al.* (2013a) and a discussion about the importance of considering Jeffrey's parameter (in the work of Tarantola (2005) appendix 6.2).

From pit measurements and first inversion trials, we can form a first insight into the range of EC and we can use a sensitivity analysis. Indeed, with $h = 0{\cdot}8$ m, we numerically obtain

$$\begin{cases} R_V = \dfrac{1}{\sqrt{4h^2+1}} = \dfrac{1}{\sqrt{4(0.8)^2+1}} \cong 0.53 \\ R_H = \sqrt{4h^2+1} - 2h \cong 0.29 \end{cases} \quad (5)$$

and

$$\begin{cases} \sigma_a^V = 0.47\sigma_1 + 0.53\sigma_2 \\ \sigma_a^H = 0.71\sigma_1 + 0.29\sigma_2 \end{cases} \quad (6)$$

It shows that, for the vertical mode, 53% of the apparent EC results from σ_2 and 47% from σ_1. If we give typical values of 2 and 20 mS m^{-1} to the two conductivities σ_1 and σ_2, respectively, it shows that the contribution of the second layer is at least 10 times that of the first layer, whereas the ratio is about 4 in the horizontal mode. The sensitivity of the measurement in the vertical dipole mode to the conductivities below 2 m is reduced to $R_V(2) = \frac{1}{\sqrt{17}} \cong 0.24\%$. In the rest of the study, we consider that the inverted second layer EC is representative of the conductivity between 0·8 and approximately 2 m.

Conversion of the electrical conductivity into clay content

Soil EC can be divided into two types, linked to the amount of water and clay content (Revil and Glover, 1997, 1998; Leroy and Revil, 2004). The first type is a bulk conductivity related to Archie's law, and the second type is a surface conductivity linked to the water trapped by clay. Following this distinction, and according to Frohlich and Parke (1989), the effective conductivity (which is also the apparent conductivity as determined by the device) can be written as

$$\sigma_{\mathrm{eff}} = \frac{\sigma_{\mathrm{water}}}{a}\Theta^k + \sigma_{\mathrm{surface}} \quad (7)$$

where σ_{water} is the EC of the water, Θ the (mobile) volumetric water content, a is a factor reflecting the influence of mineral grains on current flow and $\sigma_{surface}$ is the surface EC related to the clay content. Mualem and Friedman (1991) propose a similar relation, setting $k = 2{\cdot}5$ and involving the porosity ϕ:

$$\sigma_{eff} = \frac{\sigma_{water}}{\phi}\Theta^{2.5} + \sigma_{surface} \quad (8)$$

The volumetric water content is classically linked to the saturation (S_w) and porosity (ϕ) through Archie's law where n is the saturation exponent and m is the cementation exponent of the rock:

$$\Theta^k = S_w^n \phi^m \quad (9)$$

In the dry season, when the water content is very low, two cases may arise: (i) there is almost no clay, and the EC is residual and very low (below 5 mS m^{-1}); (ii) clays are significantly present, and we can assume the observed EC is due to the particles' surface conductivity only. In formula (7) or (8), it is not certain whether the observed residual is due to a residual amount of water or due to a small amount of clay. However, when no mobile water is available, the residual conductivity is a surface conductivity. This alternative issue has no major consequence in the present study.

To convert the EC into clay content, we can use the conversion formula given by Rhoades *et al.* (1989):

$$C = \frac{\sigma_{\mathrm{surface}} + 2.1}{2.3} \quad (10)$$

$\sigma_{surface}$ is given in mS m^{-1} (instead of mS cm^{-1} in the original formula), and clay content C in % (instead of decimals). From this formula, the amount of clay of 5% (resp. 20%) leads to a conductivity of 10 mS m^{-1} (resp. 40 mS m^{-1}).

Tree mapping

All acacias were mapped using a differential global positioning system giving an accurate position of 5 cm in all three coordinates *X*, *Y* and *Z*. Regular grids of 10 × 50 m (allowing scanning of the area and mapping of the smallest seedlings) were delimited to map all acacias. Acacias were separated into different size classes according to Grellier *et al.* (2013b) and the following criteria used: the height of 'tall' acacias was >3 m. The height of 'medium' acacias ranged between 1 and 3 m. The height of 'small' acacias was between 0·2 and 1 m. *Acacia* seedlings were <0·2 m high. *Acacia* density was calculated for each size class by counting trees in 5 × 5 m squares centred on each value of EC using ArcGis 9.3 (ESRI, 2008).

Data analysis

We tested whether the location of *Acacia* trees is spatially correlated with soil EC at 0·8- to 2m depth by using the Spatial Kolmogorov–Smirnov test of complete spatial randomness included in the package Spatstat (Baddeley and Turner, 2005) in R software version 3.0.1 (R Development Core Team 2010, http://www.R-project.org). Soil EC was log transformed prior to statistical analyses.

From the results we obtained, especially for medium-sized acacias, we found that EC might affect local maximum densities of acacias. Thus, we calculated the maximum *Acacia* density for all successive 1mS intervals of EC values. Correlations between maximum *Acacia* density and EC were tested with general additive models in R.

RESULTS

Electrical conductivity map and clay content

In the dry season, the EC of the upper layer, σ_1 (inverted by the Bayesian scheme), was $1{\cdot}5 \pm 0{\cdot}5$ mS m^{-1}. The low dispersion reveals the accuracy we have reached in the inversion, likely because of a special calibration procedure described by Grellier *et al.* (2013a). Because the accuracy we expected from Slingram data was not better that 1 mS m^{-1}, σ_1 was on the order of the detection limit of the instrument. The map of σ_1 does not carry any other significant information and is not presented here.

Electrical conductivity of the lower layer, σ_2, lies between 6 and 44 mS m^{-1} (Figure 3). The wet season case, represented in Figure 4, is provided for comparison. As previously stated, we consider that the most conductive areas in the dry season (Figure 3) reflect the presence of clay. Values of clay in the dry season, calculated with Equation (10), lie between 3 and 20% (Figure 3). We can suppose that the amount of clay derived may be affected by uncertainties that are difficult to estimate, and suggest viewing this clay content as semi-quantitative.

Acacia spatial distribution according to size classes

The four size classes of acacias showed different distribution patterns (Figure 4). Tall acacias were mostly located in the south-eastern part and in the north-western part of the plot (Figure 4a). Medium acacias followed the same pattern as tall acacias but with a higher density of trees in the north-western and central parts (Figure 4b). Small acacias had also a high density in the north-western part and central part (Figure 4c). Seedlings were more regularly dispersed on the plot with a high density in the north-eastern part of the plot, unlike other size classes (Figure 4d).

Relationship between Acacia spatial distribution and electrical conductivity (clay content) of the lower horizon

The results obtained with the complete spatial randomness test indicate that trees, independent of their size, showed a significant negative correlation with the EC or clay content of the lower horizon (Table I). All sizes, except tall acacias, had individually a significant negative correlation with EC (p-values lower than 0·05). However, tall acacias' density presented a clear threshold, with an absence of tall trees for EC higher than 24 mS m^{-1} or 12% of clay (Figures 5a and 6a). The mean value of EC where tall acacias were present was 15·7 ±4 mS m^{-1} (about 7% of clay). The EC values above these thresholds were found in the north-eastern part of the plot where EC reflects a higher clay amount in the lower layer (personal observations, unpublished data).

Medium acacias did not show as clear a threshold as tall acacias but showed a decrease of the maximal density with an increase of EC (Figure 6b). The general additive model used on the maximal densities of medium acacias and EC values was highly significant ($F = 18{\cdot}74$, $p < 0{\cdot}0001$) and explained 82·7% of the deviance in maximum medium *Acacia* density (Figure 7). Small acacias showed a less clear threshold than taller acacias, but their average densities dropped below 10 trees 100 m^{-2} for EC values above 24 mS m^{-1} (Figure 6c). No pattern could be clearly observed for seedlings (Figure 6b).

DISCUSSION

The map of soil EC showed spatial variations within our 1·5ha plot. In our study, EC can be related mainly to soil

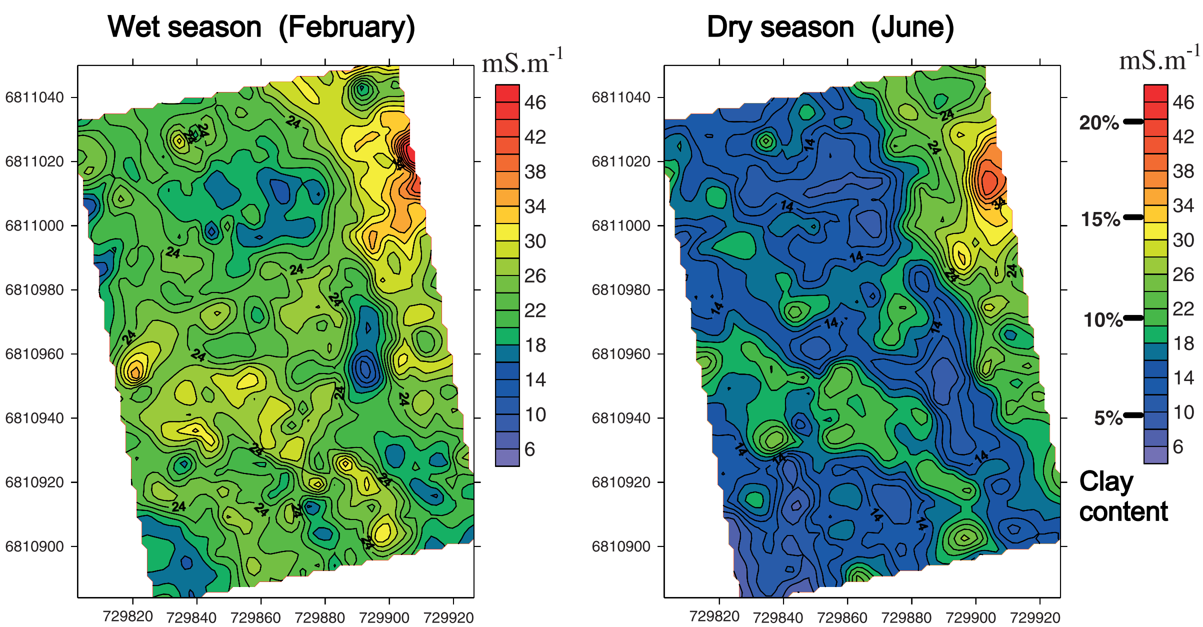

Figure 3. Electrical conductivity maps of the second layer, between 0·8 m and 2 m depths obtained with EM38-MK2, after Bayesian inversion in wet and dry season on the 1·5 ha plot. Clay content (%) is represented on the colour scale for the dry season map. Coordinate system is UTM 35 J (North upward).

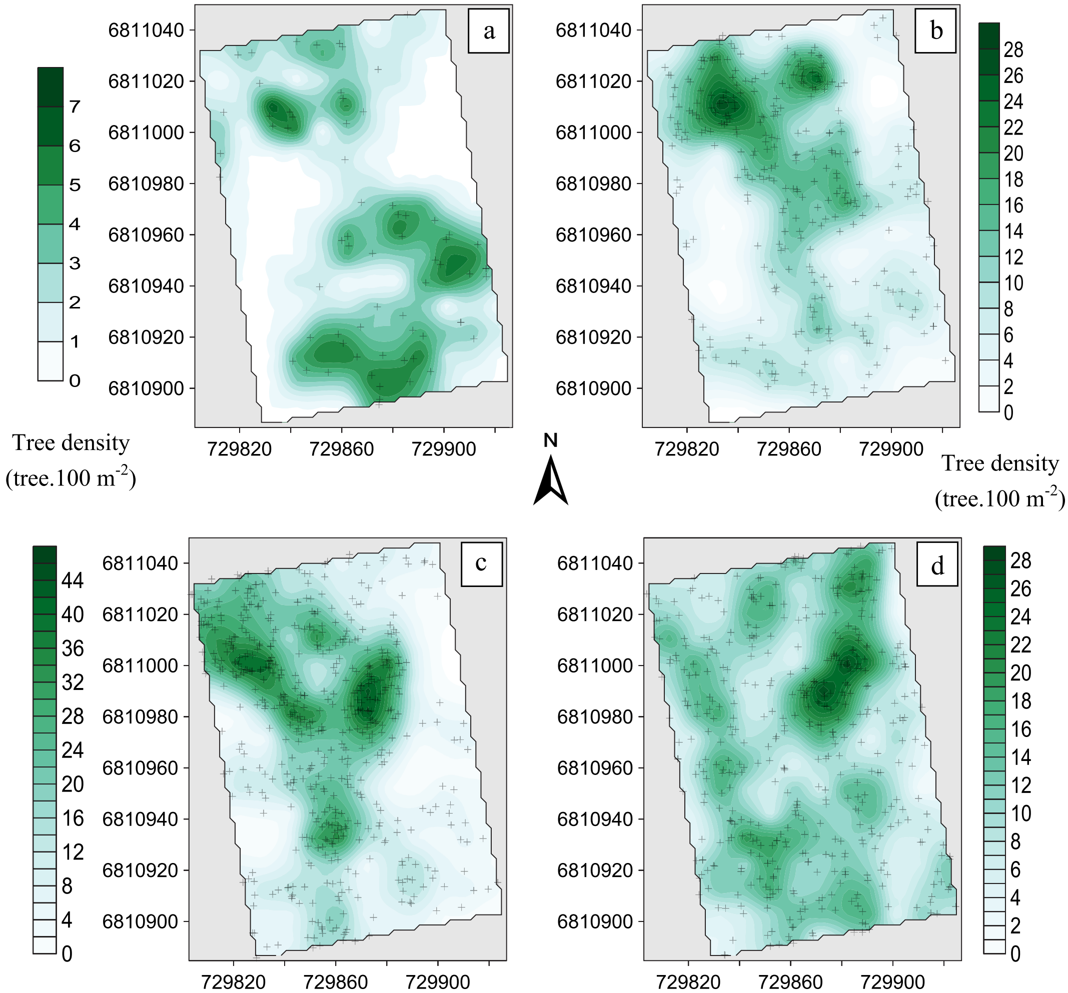

Figure 4. *Acacia* density map for each size class. (a) tall acacias; (b) medium acacias; (c) small acacias; (d) seedlings. Crosses represent each *Acacia*.

Table I. Outputs from the Spatial Kolmogorov–Smirnov test of Complete Spatial Randomness (*D*-value) and the associated *p*-value on the spatial correlation between electrical conductivity values and tree locations.

Tree size	*D*	*p*	
Seedling	0·09	0·0019	*
Small	0·10	<0·0001	**
Medium	0·11	0·0025	*
Tall	0·15	0·0733	ns
All sizes	0·07	<0·0001	**

'ns' means not significant.
Stars indicate significant *p*-values:
*$p < 0{\cdot}01$
**$p < 0{\cdot}001$

texture (clay content). This hypothesis, viz., that clay is the main factor that influences EC values during the dry season, is ascribed to Corwin and Lesch (2005). It is valid only for non-saline soils. Using this approach, it has been shown that soil texture can vary spatially according to topography (Rosenbloom *et al*., 2001) and landscape (Robinson *et al*., 2010). It was also the case in our study. In this grassland, clay content of the lower layer (0·8–2 m) is highly variable. This layer is composed of a mixture of Pleistocenic colluvium that is very heterogeneous in thickness and grain-size composition. This layer overlays a weathered Permo-Triassic parent material that is composed of a mixture of mudstone and sandstone having very different grain-size contents. This layer is also mixed with the product of weathering of metric intrusions of dolerite that is not visible at the soil surface.

The correlations between *Acacia* densities and conductivities are consistent with the study of Robinson *et al*. (2010) regarding oaks growing in semi-arid areas near Stanford (California, USA). They showed that oaks in this savanna developed preferentially on soils with lower EC in the uppermost 1 m (~21 mS m^{-1}) associated with lower clay content than areas where only grass was present (~32 mS m^{-1}).

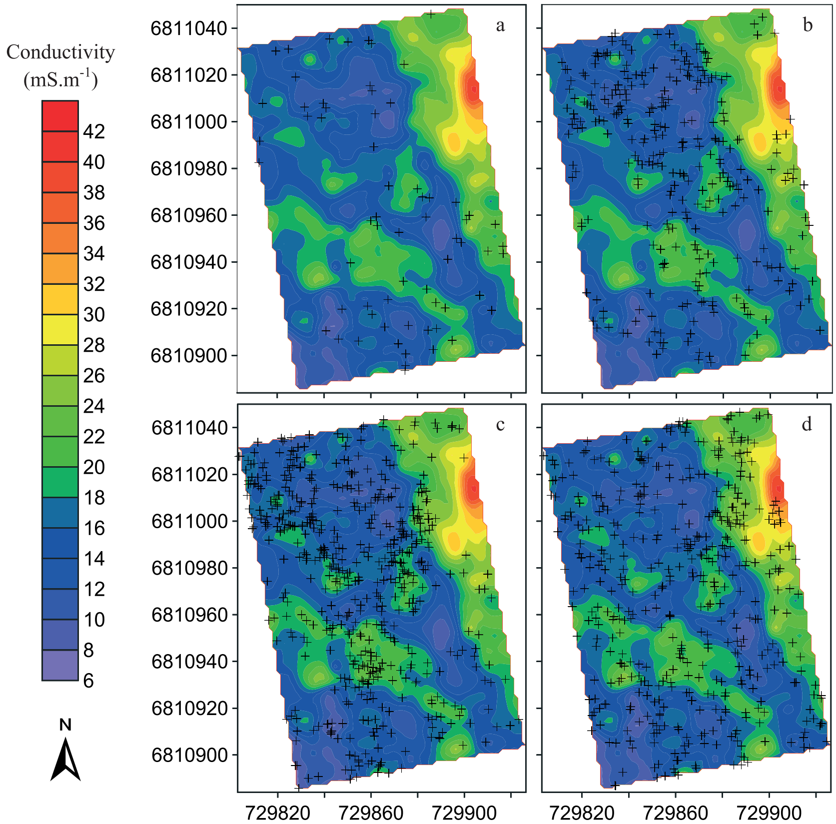

Figure 5. Electrical conductivity maps on the 1·5 ha in dry season with localization of acacias of each size classes (one black cross represents one tree). (a) Tall acacias; (b) medium acacias; (c) small acacias; (d) seedlings.

In our study, taller acacias with their deeper roots showed a net threshold of EC (or clay content) that limited their development (e.g. Figure 6). The non-significant p-value for the correlation between tall trees and conductivity ($p = 0{\cdot}073$) may be due to limited sample size (i.e. a low number of trees compared with other size classes). However, we believe that the threshold is very clear and cannot be ignored. Conductivities depend on soil properties (McNeill, 1992; Lesch and Corwin, 2003), making the comparison of absolute values between two different sites difficult.

Overall, medium and small acacias followed the same pattern as tall acacias but were not completely absent from the area of high EC, which supports our main conclusion of an effect of soil properties on the spatial distribution of trees. Presumably, seedlings with their shallower roots were not affected by the high clay content in layers at 0·8- to 2m depth as clearly as were other size classes of trees. Differences in the mortality of tree size classes may explain this pattern (Barot *et al*., 1999).

A general question arises from the type of correlative study we have used: is the spatial distribution of trees influenced by soil properties or are soil properties influenced by the presence of trees? Indeed, trees may have an impact on soil properties, especially on soil water content because trees take up water from the soil, intercept water and modify its infiltration in the soil (Liang *et al*., 2009). Alternatively, trees can move water from deeper layers to shallower layers by hydraulic lift (Ludwig *et al*., 2003) or even use inverse hydraulic lift (Schulze *et al*., 1998). Tree roots may favour soil structure and internal drainage. However, (i) we have focused on EC measurement in a dry season, which is mostly related to clay content, and (ii) trees unlikely modify soil clay content.

High clay concentrations may have negative impacts on *Acacia* development. Several studies have identified soil type as influencing tree populations either at the seedling stage (Kambatuku *et al*., 2011), or for the whole population (Schleicher *et al*., 2011). Clayey soils have a fine soil texture, which determines the porosity, the saturated hydraulic conductivity and available soil moisture for plants (Saxton *et al*., 1986; Fernández-Illescas *et al*., 2001; Fravolini *et al*., 2005). Fine-textured soils, in contrast to coarse-textured soils, have smaller pores and limit the drainage of water. This is especially true for two-layered soils with an upper sandier layer and a second more clayey layer, sometimes promoting water-logging at the surface of the less permeable second layer (Cox and McFarlane, 1995). In very fine-textured soils, tree roots may not grow as deep as in coarse-textured soils (Xu and Li, 2008; Macinnis-Ng *et al*., 2010), limiting tree growth. Although

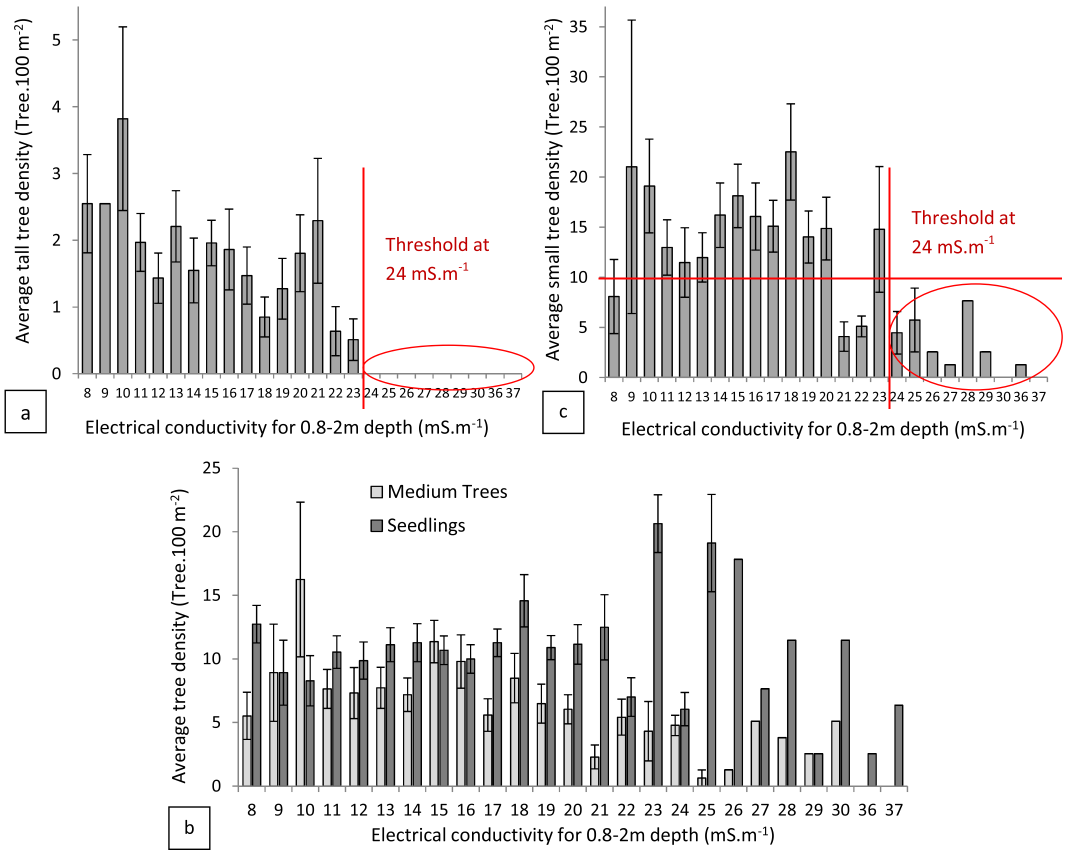

Figure 6. Average *Acacia* densities (trees 100 m^{-2}) and standard errors for soil electrical conductivities (EC) (mS m^{-1}) with a step of 1 mS m^{-1}. Note the absence of EC values between 31 and 35 mS m^{-1}. (a) Tall acacias; (b) medium acacias and seedlings; (c) small acacias.

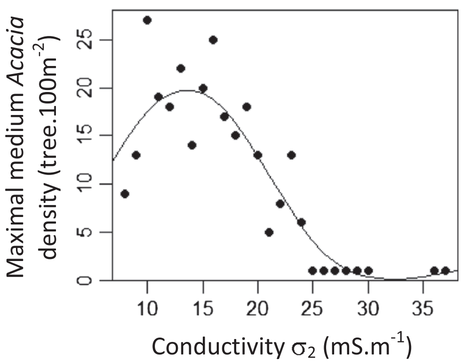

Figure 7. Maximum values of medium *Acacia* density (trees 100 m^{-2}) versus soil electrical conductivity (mS m^{-1}). The best fit curve (black line) was estimated by general additive models.

clay can have positive effects on nutrients and water availability (Bechtold and Naiman, 2006), which may favour the growth of trees or their roots (Mordelet *et al.*, 1996; Barot *et al.*, 1999), high clay content can also limit access to water for trees and thus limit their development (Xu and Li, 2008). Reduced aeration in soil with high clay content may also explain our results and are supported by the presence of lepidocrocite, which is often hydromorphic. Grass and smaller trees do not face this problem to the same extent because they mainly explore and share the uppermost layer (Kambatuku *et al.*, 2013), which is more permeable, with larger pores and with more available water (Chittleborough, 1992; Gregory *et al.*, 1992).

It would have been interesting to link the clay content directly to the hydraulic conductivities. However, the literature provides very few suitable correlations between these parameters, and generally, the correlation is not well established. Nevertheless, and taking into account the likely porosity of the sandy but consolidated colluvium on the site, we can expect that the medium becomes fully impermeable once the mineralogical clay amount reaches 20%. This may be because the available porosity could be reduced under humid conditions by the swelling properties of the clay precisely located in the colluvium deposits. These specific properties are currently under investigation at IRD Bondy, France.

CONCLUSIONS

This study showed that soil properties, and especially clay content, at depths of 0·8–2 m can drive the spatial distribution of different size classes of *A. sieberiana* in grasslands. Plot replication and/or studies at larger spatial scales with a focus on spatial relationships between size classes of trees could be interesting to further support our conclusions. This could also increase our capacity to predict tree encroachment. Together with fire, herbivory and climate, soil properties will have to be taken into account to elucidate the functioning of woody plant encroachment in grassland or savanna. Moreover, measures to control encroachment could be more effective by focusing specifically on areas that present favourable conditions for tree development. Finally, these results confirm that developing and using geophysical tools in ecology allows study at a large spatial scale without disturbing the environment and, furthermore, reveal important ecological processes.

ACKNOWLEDGEMENTS

We would like to acknowledge the NRF, SAFE Water project and the Institute of Research and Development (IRD) for funding this study. We also would like to thank Pauline Ferry, Gonca Okay and Sibonelo Mabaso for their help on the field. We further thank the Potshini Community for its support and the use of their land.

REFERENCES

Archer S. 1995. Tree-grass dynamics in a *Prosopis*-thornscrub savanna parkland: reconstructing the past and predicting the future. *Ecoscience* **2**: 83–99.

Baddeley A, Turner R. 2005. Spatstat: an R package for analyzing spatial point patterns. *Journal of Statistical Software* **12**: 1–42.

Barot S, Gignoux J, Menaut J-C. 1999. Demography of a savanna palm tree: predictions from comprehensive spatial pattern analyses. *Ecology* **80**: 1987–2005.

Bechtold SJ, Naiman RJ. 2006. Soil texture and nitrogen mineralization potential across a riparian toposequence in a semi-arid savanna. *Soil Biology and Biochemistry* **38**: 1325–1333.

Bond WJ, Midgley JJ. 2000. A proposed CO2-controlled mechanism of woody plant invasion in grasslands and savannas. *Global Change Biology* **6**: 865–869.

Botha GA, Wintle AG, Vogel JC. 1994. Episodic late Quaternary palaeogully erosion in northern KwaZulu-Natal, South Africa. *Catena* **23**: 327–340.

Britz M-L, Ward D. 2007. The effects of soil conditions and grazing strategy on plant species composition in a semi-arid savanna. *African Journal of Range & Forage Science* **24**: 51–61.

Brown JR, Archer S. 1999. Shrub invasion of grassland: recruitment is continuous and not regulated by herbaceous biomass or density. *Ecology* **80**: 2385–2396.

Browning DM, Archer SR, Asner GP, McClaran MP, Wessman CA. 2008. Woody plants in grasslands: post-encroachment stand dynamics. *Ecological Applications* **18**: 928–944.

Callaway RM, Walker LR. 1997. Competition and facilitation: a synthetic approach to interactions in plant communities. *Ecology* **78**: 1958–1965.

Chittleborough DJ. 1992. Formation and pedology of duplex soils. *Australian Journal of Experimental Agriculture* **32**: 815–825.

Cockx L, Van Meirvenne M, De Vos B. 2007. Using the EM38DD soil sensor to delineate clay lenses in a sandy forest soil. *Soil Science Society of America Journal* **71**: 1314–1322. DOI: 10.2136/sssaj2006.0323

Colgan MS, Asner GP, Levick SR, Martin RE, Chadwick OA. 2012. Topo-edaphic controls over woody plant biomass in South African savannas. *Biogeosciences* **9**: 1809–1821. DOI: 10.5194/bg-9-1809-2012

Corwin DL, Lesch SM. 2005. Apparent soil electrical conductivity measurements in agriculture. *Computers and Electronics in Agriculture* **46**: 11–43.

Cox JW, McFarlane DJ. 1995. The causes of waterlogging in shallow soils and their drainage in southwestern Australia. *Journal of Hydrology* **167**: 175–194.

Eggemeyer KD, Schwinning S. 2009. Biogeography of woody encroachment: why is mesquite excluded from shallow soils? *Ecohydrology* **2**: 81–87.

ESRI. 2008. ArcMap-ArcEditor version 9.3, Environmental Systems Research Institute, Inc.

FAO. 1998. *World Reference Base for Soil Resources*. World Soil Resources Reports, FAO: Rome, Italy.

Fernández-Illescas CP, Porporato A, Laio F, Rodríguez-Iturbe I. 2001. The ecohydrological role of soil texture in a water-limited ecosystem. *Water Resource Research* **37**: 2863–2872.

Fravolini A, Hultine KR, Brugnoli E, Gazal R, English NB, Williams DG. 2005. Precipitation pulse use by an invasive woody legume: the role of soil texture and pulse size. *Oecologia* **144**: 618–627.

Frohlich RK, Parke CD. 1989. The electrical resistivity of the vadose zone – field survey. *Ground Water* **27**: 524–530.

Graz FP. 2008. The woody weed encroachment puzzle: gathering pieces. *Ecohydrology* **1**: 340–348.

Gregory PJ, Tennant D, Hamplin AP, Eastham J. 1992. Components of the water-balance on duplex soils in western Australia. *Australian Journal of Experimental Agriculture* **32**: 845–855.

Grellier S. 2011. *Hillslope Encroachment by Acacia Sieberiana in a Deep-Gullied Grassland of KwaZulu-Natal (South Africa)*. PhD thesis. University of Pierre and Marie Curie: Paris, France.

Grellier S, Janeau J-L, Barot S, Ward D. 2012a. Grass competition is more important than seed ingestion by livestock for *Acacia* recruitment in South Africa. *Plant Ecology* **213**: 899–908.

Grellier S, Kemp J, Florsch N, Janeau J-L, Ward D, Barot S, Podwojewski P, Lorentz S, Valentin C. 2012b. The indirect impact of encroaching trees on gully extension: a 64 year study in a sub-humid grassland of South Africa. *Catena* **98**: 110–119.

Grellier S, Florsch N, Camerlynck C, Janeau JL, Podwojewski P, Lorentz S. 2013a. The use of Slingram EM38 data for topsoil and subsoil geoelectrical characterization with a Bayesian inversion. *Geoderma* **200-201**: 140–155.

Grellier S, Ward D, Janeau J-L, Podwojewski P, Lorentz S, Abbadie L, Valentin C, Barot S. 2013b. Positive versus negative environmental impacts of tree encroachment in South Africa. *Acta Oecologica* **53**: 1–10. http://dx.doi.org/10.1016/j.actao.2013.08.002

Halpern CB, Antos JA, Rice JM, Haugo RD, Lang NL. 2010. Tree invasion of a montane meadow complex: temporal trends, spatial patterns, and biotic interactions. *Journal of Vegetation Science* **21**: 717–732.

Hezarjaribi A, Sourell H. 2007. Feasibility study of monitoring the total available water content using non-invasive electromagnetic induction-based and electrode-based soil electrical conductivity measurements. *Irrigation and Drainage* **56**: 53–65.

Hossain MB, Lamb DW, Lockwood PV, Frazier P. 2010. EM38 for volumetric soil water content estimation in the root-zone of deep vertosol soils. *Computers and Electronics in Agriculture* **74**: 100–109.

Kambatuku JR, Cramer MD, Ward D. 2011. Savanna tree–grass competition is modified by substrate type and herbivory. *Journal of Vegetation Science* **22**: 225–237.

Kambatuku JR, Cramer MD, Ward D. 2013. Overlap in soil water sources of savanna woody seedlings and grasses. *Ecohydrology* **6**: 464–473. DOI: 10.1002/eco.1273

King GM. 2002. *An Explanation of the 1:500 000 General Hydrogeological Map*. Department of Water Affairs and Forestry: Pretoria, South Africa.

Lata JC, Degrange V, Raynaud X, Maron PA, Lensi R, Abbadie L. 2004. Grass populations control nitrification in savanna soils. *Functional Ecology* **18**: 605–611. DOI: 10.1111/j.0269-8463.2004.00880.x

Leroy P, Revil A. 2004. A triple-layer model of the surface electrochemical properties of clay minerals. *Journal of Colloid and Interface Science* **270**: 371–380. DOI: 10.1016/j.jcis.2003.08.007

Lesch SM, Corwin DL. 2003. Using the dual-pathway parallel conductance model to determine how different soil properties influence conductivity survey data. *Agronomy Journal* **95**: 365–379.

Liang W-L, Kosugi K, Mizuyama T. 2009. A three-dimensional model of the effect of stemflow on soil water dynamics around a tree on a hillslope. *Journal of Hydrology* **366**: 62–75.

Ludwig F, Dawson TE, de Kroon H, Berendse F, Prins HHT. 2003. Hydraulic lift in *Acacia tortilis* trees on an East African savanna. *Oecologia* **134**: 293–300.

Macinnis-Ng CMO, Fuentes S, O'Grady AP, Palmer AR, Taylor D, Whitley RJ, Yunusa I, Zeppel MJB, Eamus D. 2010. Root biomass distribution and soil properties of an open woodland on a duplex soil. *Plant and Soil* **327**: 377–388.

McNeill JD. 1980. *Electromagnetic Terrain Conductivity Measurement at Low Induction Numbers, Tech. Note TN-6*. Geonics Ltd: Mississauga, Ontario. http://www.geonics.com/pdfs/technicalnotes/tn6.pdf

McNeill JD. 1992. Rapid, accurate mapping of soil salinity by electromagnetic ground conductivity meters. *in Advances in Measurement of Soil Physical Properties: Bringing Theory Into Practice, Specific Publication 30, Soil Science Society of America, Madison, Wisconsin*, 209–229.

Meyer KM, Wiegand K, Ward D, Moustakas A. 2007. SATCHMO: a spatial simulation model of growth, competition, and mortality in cycling savanna patches. *Ecological Modelling* **209**: 377–391.

Mordelet P, Barot S, Abbadie L. 1996. Root foraging strategies and soil patchiness in a humid savanna. *Plant and Soil* **182**: 171–176.

Mualem Y, Friedman S. 1991. Theoretical prediction of electrical conductivity in saturated and unsaturated soil. *Water Ressources Research* **27**: 2771–2777. DOI: 10.1029/91WR01095

Mucina L, Rutherford MC. 2006. *The Vegetation of South Africa, Lesotho and Swaziland*. Strelitzia 19, South African National Biodiversity Institute: Pretoria, South Africa.

Myers DB, Kitchen NR, Sudduth KA, Sharp RE, Miles RJ. 2007. Soybean root distribution related to claypan soil properties and apparent soil electrical conductivity. *Crop Science* **47**: 1498–1509. DOI: 10.2135/cropsci2006.07.0460

Revil A, Glover PWJ. 1997. Theory of ionic-surface electrical conduction in porous media. *Physical Review B* **55**: 1757–1773. DOI: 10.1103/PhysRevB.55.1757

Revil A, Glover PWJ. 1998. Nature of surface electrical conductivity in natural sands, sandstones, and clays. *Geophysical Research Letters* **25**: 691–694. DOI: 10.1029/98gl00296

Rhoades J, Manteghi N, Shrouse P, Alves W. 1989. Soil electrical conductivity and soil salinity: new formulations and calibrations. *Soil Science Society of America Journal* **53**: 433–439.

Robinson DA, Abdu H, Jones SB, Seyfried M, Lebron I, Knight R. 2008. Eco-geophysical imaging of watershed-scale soil patterns links with plant community spatial patterns. *Vadose Zone Journal* **7**: 1132–1138.

Robinson DA, Lebron I, Querejeta JI. 2010. Determining soil–tree–grass relationships in a california oak savanna using eco-geophysics. *Vadose Zone Journal* **9**: 1–8.

Rosenbloom NA, Doney SC, Schimel DS. 2001. Geomorphic evolution of soil texture and organic matter in eroding landscapes. *Global Biogeochemistry Cycles* **15**: 365–381.

Sankaran M, Ratnam J, Hanan NP. 2004. Tree–grass coexistence in savannas revisited – insights from an examination of assumptions and mechanisms invoked in existing models. *Ecology Letters* **7**: 480–490.

Sankaran M, Hanan NP, Scholes RJ, Ratnam J, Augustine DJ, Cade BS, Gignoux J, Higging SI, Roux XL, Ludwig F, Ardo J, Banyikwa F, Bronn A, Bucini G, Caylor KK, Coughenour MB, Diouf A, Ekaya W, Feral CJ, February EC, Frost PGH, Hiernaux P, Hrabar H, Metzger KL, Prins HHT, Ringrose S, Sea W, Tews J, Worden J, Zambatis N. 2005. Determinants of woody cover in African savannas. *Nature* **438**: 846–849.

Sankaran M, Ratnam J, Hanan N. 2008. Woody cover in African savannas: the role of resources, fire and herbivory. *Global Ecology and Biogeography* **17**: 236–245.

Saxton K, Rawls WJ, Romberger JS, Ri P. 1986. Estimating generalized soil water characteristics from texture. *Soil Science Society of America Journal* **50**: 1031–1036.

Schleicher J, Wiegand K, Ward D. 2011. Changes of woody plant interaction and spatial distribution between rocky and sandy soil areas in a semi-arid savanna, South Africa. *Journal of Arid Environments* **75**: 270–278.

Schulze E-D, Caldwell MM, Canadell J, Mooney HA, Jackson RB, Parson D, Scholes R, Sala OE, Trimborn P. 1998. Downward flux of water through roots (i.e. inverse hydraulic lift) in dry Lalahari sands. *Oecologia* **115**: 460–462.

Tarantola A. 2005. *Inverse Problem Theory and Methods for Model Parameter Estimation*. Society for Industrial and Applied Mathematics: Philadelphia, PA, U.S.A.

Tarantola A, Valette B. 1982a. Generalized nonlinear inverse problems solved using the least square criterion. *Reviews of Geophysics and Space Physics* **20**: 219–232.

Tarantola A, Valette B. 1982b. Inverse problems – quest for information. *Journal of Geophysics* **50**: 159–170.

Van Auken OW. 2009. Causes and consequences of woody plant encroachment into western North American grasslands. *Journal of Environmental Management* **90**: 2931–2942.

Verboom WH, Pate JS. 2013. Exploring the biological dimension to pedogenesis with emphasis on the ecosystems, soils and landscapes of southwestern Australia. *Geoderma* **211**: 154–183. DOI: 10.1016/j.geoderma.2012.03.030

Wang YQ, Shao MA, Liu ZP, Warrington DN. 2012. Regional spatial pattern of deep soil water content and its influencing factors. *Hydrological Sciences Journal-Journal Des Sciences Hydrologiques* **57**: 265–281. DOI: 10.1080/02626667.2011.644243

Ward D. 2005. Do we understand the causes of bush encroachment in African savannas? *African Journal of Range & Forage Science* **22**: 101–105.

Ward D. 2010. A resource ratio model of the effects of changes in CO_2 on woody plant invasion. *Plant Ecology* **209**: 147–152.

Weng ES, Luo YQ. 2008. Soil hydrological properties regulate grassland ecosystem responses to multifactor global change: a modeling analysis. *Journal of Geophysical Research-Biogeosciences* **113**: DOI: 10.1029/2007jg000539

Wiegand K, Ward D, Saltz D. 2005. Multi-scale patterns and bush encroachment in an arid savanna with a shallow soil layer. *Journal of Vegetation Science* **16**: 311–320.

Wiegand K, Saltz D, Ward D. 2006. A patch-dynamics approach to savanna dynamics and woody plant encroachment – insights from an arid savanna. *Perspectives in Plant Ecology, Evolution and Systematics* **7**: 229–242.

Xu GQ, Li Y. 2008. Rooting depth and leaf hydraulic conductance in the xeric tree Haloxyolon ammodendron growing at sites of contrasting soil texture. *Functional Plant Biology* **35**: 1234–1242.

Young MH, Robinson DA, Ryel RJ. 2010. Introduction to coupling soil science and hydrology with ecology: toward integrating landscape processes. *Vadose Zone Journal* **9**: 515–516.

